

Total Anomalous Pulmonary Venous Connection in Children:

Preoperative Evaluation with Low-Dose Multidetector Computed Tomographic Angiography

Aysel Turkvatan, MD
Hasan Tahsin Tola, MD
Pelin Ayyildiz, MD
Erkut Ozturk, MD
Yakup Ergul, MD
Alper Guzeltas, MD

Key words: Angiography/methods; child, preschool; cardiovascular anomalies/diagnosis/diagnostic imaging; heart defects, congenital/complications/diagnostic imaging; pulmonary veins/abnormalities/diagnostic imaging/pathology; radiation dosage; radiographic image interpretation, computer-assisted; retrospective studies; tomography, x-ray computed/methods

From: Departments of Radiology (Dr. Turkvatan) and Pediatric Cardiology (Drs. Ayyildiz, Ergul, Guzeltas, Ozturk, and Tola), Istanbul Mehmet Akif Ersoy Thoracic and Cardiovascular Surgery Training and Research Hospital, Istanbul 34307, Turkey

Address for reprints:
Aysel Turkvatan, MD,
Department of Radiology,
11 Istanbul St., Kucukcekmece, Istanbul 34307,
Turkey

E-mail:
aturkvatan@yahoo.com

© 2017 by the Texas Heart®
Institute, Houston

We report the results of our retrospective evaluation, from February 2011 through August 2014, of the anatomic features of total anomalous pulmonary venous connection (TAPVC) and its associated cardiovascular anomalies in a pediatric population. In all 43 patients under study (23 female; average age, 9 mo [range, 4 d–7.1 yr]), these examinations had been performed with a dual-source 256-detector scanner.

The type of TAPVC, the presence of obstruction, and the association with other cardiovascular anomalies were investigated and recorded. In accordance with the absence or presence of these accompanying anomalies, patients were subdivided into 2 groups: isolated and complex.

In the 43 patients, 22 (51%) TAPVCs were supracardiac, 10 (23%) were cardiac, 6 (14%) were infracardiac, and 5 (12%) were mixed. Obstruction was detected in 7 patients. Seventeen patients were in the isolated group and 26 in the complex group. The diagnostic agreements between multidetector computed tomographic angiographic and surgical results were 100% in both the isolated and complex groups. The overall average effective radiation dose was 0.66 mSv (range, 0.15–1.11 mSv); and it was 0.52 mSv (range, 0.12–0.72 mSv) in patients younger than 1 year of age.

We conclude that computed tomographic angiography with a dual-source 256-slice multidetector scanner is a reliable imaging method that enables, despite lower radiation doses, the detailed and comprehensive anatomic imaging of TAPVC in neonates and children. (*Tex Heart Inst J* 2017;44(2):120-6)

Total anomalous pulmonary venous connection (TAPVC) constitutes approximately 1% to 3% of all cardiovascular abnormalities in which the pulmonary veins (PVs) have no connection with the left atrium and connect directly to the right atrium or to one or more systemic veins.¹ Embryologically, TAPVC results from early atresia or failure of the common PV to develop, with persistence of at least one connection to the cardinal or the umbilical vitelline venous system.² Total anomalous pulmonary venous connection is a cause of neonatal cyanosis and can result in rapid death when blood is not shunted from the right side of the heart to the left side. Isolated TAPVC is diagnosed if the patient has atrial septal defect (ASD), patent ductus arteriosus (PDA), or both; complex TAPVC is diagnosed if the patient has other intracardiac lesions in addition to ASD or PDA. Although TAPVC is usually isolated, it can be a component of a complex cardiovascular disease such as heterotaxy syndrome.³ Accurate delineation of TAPVC and the cardiovascular anomalies that accompany it are important to the guidance of surgical planning in these patients.

Although TAPVCs have usually been evaluated with use of echocardiography and catheter angiography, magnetic resonance imaging (MRI) and multidetector computed tomographic angiography (MDCTA) are now playing larger roles in the diagnosis of these anomalies.⁴ These imaging methods help overcome the shortcomings of transthoracic echocardiography (TTE), which gives a suboptimal acoustic window and a poor depiction of extracardiac vascular structures. They are also an improvement over catheter angiography, which produces overlapping views of adjacent vascular structures, causes difficulty in the simultaneous depiction of the systemic and pulmonary vascular systems, leads to undesirable catheter-related sequelae, and delivers relatively high doses of ionizing radiation.⁵ Even though MRI is eminently

capable in the anatomic and functional evaluation of the heart, it is time-consuming and often requires lengthy sedation; therefore, the use of MRI in seriously ill or uncooperative patients is usually restricted. In recent times, MDCTA has been used more and more to evaluate patients with suspected or known congenital heart disease, especially those in whom associated vascular anomalies must be ruled out. Compared with first-generation computed tomographic (CT) scanners, multidetector CT scanners—with their high volume of coverage (≥ 128 slices/gantry rotation)—enable faster and more accurate evaluation of the cardiac and vascular anatomy, with lower radiation exposure.⁶⁻¹³

In this study, we used high-pitch, dual-source 256-slice MDCTA to evaluate the anatomic features of TAPVC and associated cardiovascular anomalies in a pediatric population, and we report the radiation doses associated with these examinations.

Patients and Methods

This study was a combined retrospective and prospective analysis of MDCTA studies performed on patients with TAPVC at a single institution from February 2011 through August 2014. We included 43 patients (23 female; average age, 9 mo [range, 4 d–7.1 yr]) with TAPVC diagnosed by MDCTA. All patients had undergone TTE and had been referred by a pediatric cardiologist for further definition of cardiac and vascular anatomy, in cases clinically indicated for MDCTA. This study was approved by the institutional review board of the hospital, and written informed consent was granted by the parents of all study participants.

We performed MDCTA examinations with use of a 2nd-generation, dual-source 256-MDCT SOMATOM® Definition Flash scanner (Siemens Healthcare GmbH; Forchheim, Germany) with a sectional collimation of $2 \times 128 \times 0.6$ mm, gantry rotation time of 280 ms, and temporal resolution of 75 ms. A nonelectrocardiographic (non-ECG) gated protocol with a pitch factor of 3 was used, and every scan in every patient was obtained via the z-axis CARE Dose modulation technique (Siemens Healthcare). The voltage and tube current were adjusted to the patient's weight as follows: 80 kV dosage was used for patients weighing < 20 kg, and 100 kV for those weighing 20 to 80 kg; tube current was 10 mA/kg for patients weighing < 9 kg, and 5 mA for each additional kg. The scan volume was extended from the base of the neck superiorly to just below the diaphragm inferiorly. In cases of suspected infracardiac TAPVC, the scan volume was extended to the inferior portion of the liver. The imaging data were acquired during an intravenous injection of 1.5 to 2 mL/kg of the contrast agent iodixanol (320 mg/mL) at a rate of 1 to 3 mL/s for children, but the drug was manually administered to neonates and infants. Contrast material was followed by 4 to 15

mL of saline solution. The scanning delay was determined with use of a bolus-tracking technique; control images in the left ventricle were positioned in an axial plane. Because the contrast material was clearly seen within the left ventricular cavity, the scan was initiated with a 2-s delay. In older children, the scan was started 7 s after the attenuation of the region of interest in the ascending aorta reached 150 Hounsfield units (HU). All the patients were in sinus rhythm, and none needed β -blockers despite heart rates that exceeded 80 beats/min in all cases. No patients needed sedation. Children younger than 5 years old were offered honey on a pacifier or a lollipop during CT acquisition. All CT acquisitions were obtained with the patients breathing freely. Images were reconstructed to 0.6 mm in thickness and to a reconstruction interval with a 25f kernel filter; they were processed on a separate *syngo.via* workstation (Siemens Healthcare) with multiplanar reformatting, maximum-intensity projection, and volume rendering. Multidetector computed tomographic images were retrospectively reviewed by 2 radiologists (with 15 and 5 years of experience in cardiovascular imaging), and decisions were made by consensus. Image quality was evaluated on a semiquantitative 5-point scale consisting of the subjective perception of image noise, soft-tissue contrast, sharpness of tissue interfaces, conspicuity of anatomic details, and degree of image degradation. A score of 5 indicated excellent image quality (no motion artifacts); 4, good image quality (discreet motion artifacts, < 2 mm); 3, moderate image quality (pronounced motion artifacts, > 2 mm); 2, suboptimal image quality; and 1, unacceptable image quality. Image quality was considered sufficient for diagnostic purposes when the score was ≥ 3 . To objectively evaluate image quality, the image noise and signal-to-noise ratios were determined on a 0.6-mm-thick axial slice by measuring the average density of contrast media and standard deviation in HU within 2 regions of interest (> 100 pixels) in the pulmonary trunk and in the middle of the ascending aorta at the same level. Each region of interest was measured 3 times, and the average value was calculated.

The type of TAPVC (supracardiac, cardiac, infracardiac, or mixed), the presence of obstruction, and associated cardiovascular anomalies were investigated. According to the accompanying cardiovascular anomalies, patients were subdivided into 2 groups, isolated or complex. The isolated type was diagnosed if the patient had associated ASD or PDA; the complex type of TAPVC was diagnosed if the patient had cardiovascular anomalies in addition to ASD or PDA.

The information on the patient's radiation dose was obtained from the CT system. For examination purposes, the estimated effective radiation doses (mSv) were calculated by multiplying the dose length product (mGy·cm) by a conversion coefficient ($\text{mSv} \cdot \text{mGy}^{-1} \cdot \text{cm}^{-1}$) corrected for the patient's age. This was obtained

from previously published literature (0.039 for <4 mo of age, 0.026 for 4–12 mo, 0.018 for 2–6 yr, and 0.013 for ≥ 7 yr).¹⁴

Statistical Analysis

Statistical analysis was performed with the use of SPSS 17.0 (IBM Corporation; Endicott, NY). Continuous variables were presented as mean \pm SD, or as a range. Categorical data were presented as percentages or frequencies. Interobserver agreement on semiquantitative grades of image quality was expressed by using the kappa statistic, with $\kappa \geq 0.9$ considered excellent agreement, $\kappa > 0.81$ considered strong agreement, and $\kappa = 0.61$ –0.80 considered good agreement. The accuracy of 256-slice MDCT in the evaluation of TAPVC was determined by comparing intraoperative findings.

Results

Interobserver agreement of overall image quality was reached in 42 (97.6%) studies ($\kappa > 0.81$). Disagreement occurred in one study, with only one point of difference. Diagnostic images (image quality scores, ≥ 3) were obtained in all the acquisitions (100%). The mean image-quality score was 4.2 ± 0.8 (range, 3–5). The average attenuation in both the ascending aorta and pulmonary trunk was 442 ± 118 and 440 ± 115 HU, respectively. The median noise in the ascending aorta and pulmonary trunk was 18 and 20 HU, respectively. The median signal-to-noise ratio in the ascending aorta and pulmonary trunk was 22 and 21, respectively.

The prevalent TAPVC was supracardiac in 22 (51%) patients, followed by cardiac in 10 (23%) patients, infracardiac type in 6 (14%) patients, and mixed type in 5 (12%) patients.

The MDCTA images clearly depicted the drainage sites in all patients. Among the 22 patients with supracardiac TAPVC, 12 had a connection to the left brachiocephalic vein (Fig. 1), 8 had a connection to the right superior vena cava (Fig. 2), one had a connection to the left superior vena cava, and one had a connection to the right brachiocephalic vein. In the 10 patients with cardiac TAPVC, the PVs connected to the coronary sinus in 6 patients and to the right atrium in 4 patients (Fig. 3). In the 6 patients with infracardiac TAPVC, 2 had a connection to the portal vein (Fig. 4), 2 had a connection to the inferior vena cava, one had a connection to the left hepatic vein, and one had a connection to the ductus venosus (Fig. 5). All 5 patients with mixed TAPVC had a combination of supracardiac and cardiac connections.

Obstructions were detected in 7 patients (16%). Of these obstructions, 3 were at the supradiaphragmatic level: vertical vein–left brachiocephalic vein connection, 1; common PV–superior vena cava connection, 1; and common PV–right brachiocephalic vein connection, 1. Two were at the infradiaphragmatic level: left hepatic vein–inferior vena cava connection, 1; and vertical vein–ductus venosus connection, 1. One was at the diaphragmatic level, and one was a stenotic individual PV. Of these sites of obstruction, 6 were caused by intrinsic stenosis and one by extrinsic compression of the diaphragm.

Of the 43 patients with TAPVC, 17 (40%) had the isolated type and 26 (60%) had the complex type. Among the 17 patients with the isolated type, 12 had associated ASD, 2 had associated PDA, and 3 had both. The 26 patients with complex TAPVC had, in addition to ASD or PDA, one or more of these anomalies: atrioventricular septal defect ($n=7$), ventricular septal

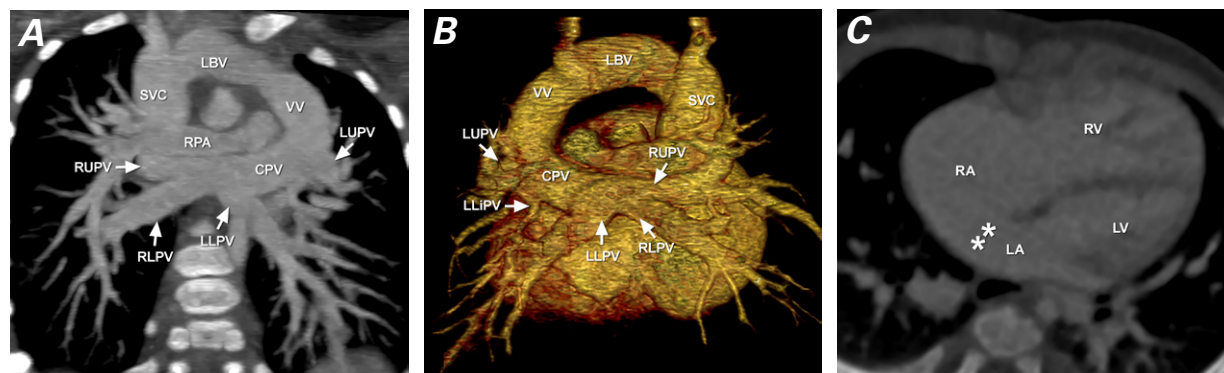


Fig. 1 Computed tomograms in a 3-month-old girl with supracardiac total anomalous pulmonary venous connection to the left brachiocephalic vein (LBV). **A)** Oblique coronal thin maximum-intensity projection and **B)** posterior volume-rendering show that all pulmonary veins drain into the common pulmonary vein (CPV), which connects to the LBV through a left-sided ascending vertical vein (VV). The LBV and superior vena cava (SVC) are dilated. **C)** Axial image reveals an associated secundum-type atrial septal defect (double asterisk).

LA = left atrium; LLiPV = left lingular pulmonary vein; LLPV = left lower pulmonary vein; LUPV = left upper pulmonary vein; LV = left ventricle; RA = right atrium; RLPV = right lower pulmonary vein; RPA = right pulmonary artery; RUPV = right upper pulmonary vein; RV = right ventricle

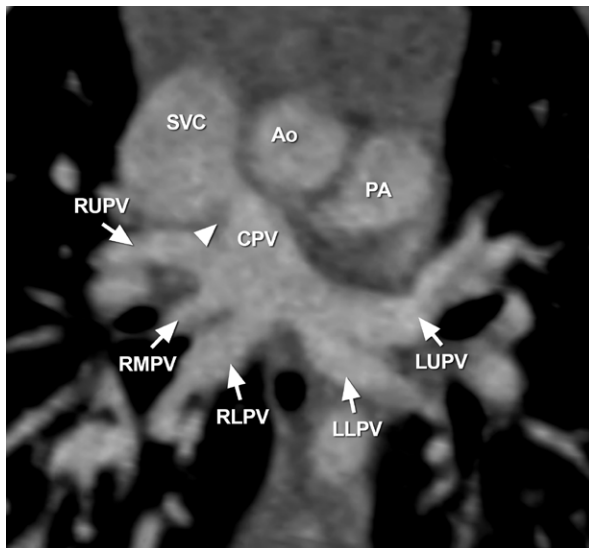


Fig. 2 Computed tomogram (oblique coronal thin maximum-intensity projection) of a 24-day-old boy shows a supracardiac total anomalous pulmonary venous connection to the right superior vena cava (SVC). All pulmonary veins drain into the common pulmonary vein (CPV), which connects to the SVC. Arrowhead indicates moderate obstruction of the CPV at the entrance to the SVC.

Ao = aorta; LLPV = left lower pulmonary vein; LUPV = left upper pulmonary vein; PA = pulmonary artery; RLPV = right lower pulmonary vein; RMPV = right middle pulmonary vein; RUPV = right upper pulmonary vein



Fig. 4 Computed tomogram (oblique coronal thin maximum-intensity projection) in a month-old girl shows an infracardiac total anomalous pulmonary venous connection to the portal vein (PoV). All pulmonary veins (asterisks) drain into the common pulmonary vein (CPV), which connects to the PoV through a descending vertical vein (VV).

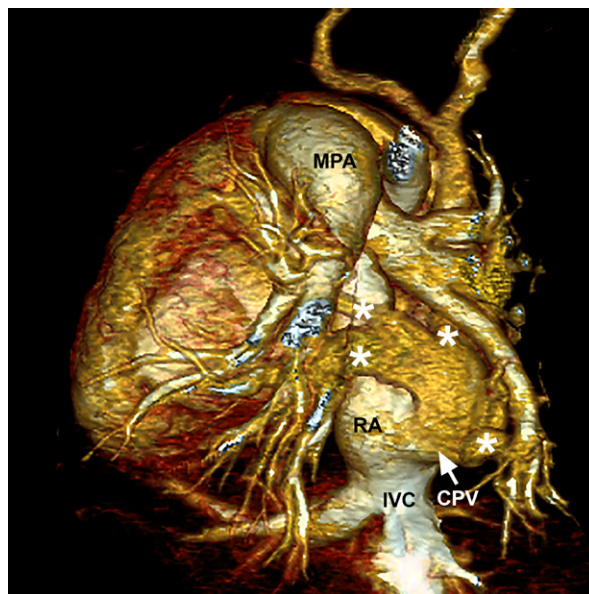


Fig. 3 Computed tomogram (oblique posterior volume-rendering) of a 2-month-old girl shows a cardiac total anomalous pulmonary venous connection to the right atrium (RA). All pulmonary veins (asterisks) drain into the common pulmonary vein (CPV) confluence posterior to the heart, which empties into the RA.

IVC = inferior vena cava; MPA = main pulmonary artery

defect (n=7), persistent left superior vena cava (n=7), pulmonary stenosis (n=7), right atrial isomerism (n=5), double-outlet right ventricle (n=5), right aortic arch (n=5), transposition of the great arteries (n=4), tubular hypoplasia of the aortic arch (n=3), aortic coarctation (n=3), pulmonary artery hypoplasia (n=3), right pulmonary artery agenesis (n=1), cor triatriatum sinister (n=1), left ventricular agenesis (n=1), pulmonary atresia (n=1), hepatic interruption and anomalous drainage of the inferior vena cava into the left atrium (n=1), and an accessory left hepatic vein anomalously draining into the left atrium (n=1).

In 40 patients (93%), TAPVC and its associated cardiovascular anomalies were corrected surgically. All the MDCTA findings (type of TAPVC, presence and location of the obstruction, and associated cardiovascular anomalies) correlated well with the intraoperative surgical findings, and no major discrepancies were noted. The diagnostic agreements between MDCTA and the surgical results were 100% in both the isolated and complex groups.

The overall average effective radiation dose for all 43 patients was 0.66 mSv (range, 0.15–1.11 mSv), and it was 0.52 mSv (range, 0.12–0.72) in those 28 patients younger than 1 year of age.

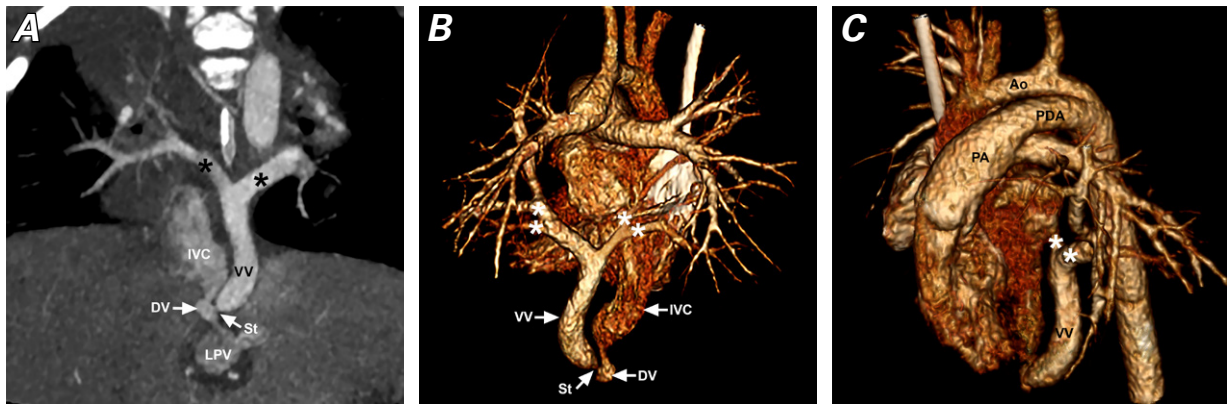


Fig. 5 Computed tomograms in a 2-month-old boy with an infracardiac total anomalous pulmonary venous connection to the ductus venosus (DV). **A**) Oblique coronal thin maximum-intensity projection and **B**) posterior volume-rendering show all pulmonary veins (asterisks) draining into a common pulmonary vein that connects to the DV through a descending vertical vein (VV). Severe stenosis (St) of the VV is seen at the entrance to the DV. Severe stenosis of the DV is also seen. **C**) Left oblique volume-rendering reveals an associated large patent ductus arteriosus (PDA).

Ao = aorta; IVC = inferior vena cava; LPV = left portal vein; PA = pulmonary artery

Discussion

In the present study, we evaluated the anatomic features and the accompanying cardiovascular anomalies of TAPVC in the pediatric population, by means of high-pitch dual-source 256-slice MDCTA. Until now, little information has been available regarding the performance of this scanner in the evaluation of pediatric patients with TAPVC. To the best of our knowledge, our series provides the largest study of pediatric TAPVC patients evaluated by means of MDCTA, with a high volume of coverage and with good interobserver agreement. It distinctly shows that high-pitch MDCTA plays an important role in evaluating the anatomic features and associated cardiovascular anomalies of TAPVC in the pediatric population, without ECG triggering. Our results indicate that high-pitch axial scanning with a tube voltage of 80 kV is the preferred scanning mode, because it results in the lowest effective radiation dose in the newborn and in infants, while maintaining a high level of diagnostic-image quality.

In patients with TAPVC, correct delineation of the anatomy and associated cardiovascular anomalies is crucial in planning treatment. Generally, TTE is regarded as an initial screening and diagnostic method in patients with TAPVC. Indeed, for most patients with isolated TAPVC, TTE as the sole preoperative imaging mode produces enough information for simple surgical repair.

However, in patients with complex TAPVC, TTE is frequently supplemented by diagnostic catheter angiography for additional anatomic and functional characterization.¹⁵ Although conventional catheter angiography has been accepted as the gold standard—and it does enable detailed evaluation of the drainage of the PVs and of possible obstructions—it carries the risk of cardiac

arrest and even of death in cases of obstructive TAPVC and severe cyanosis.¹⁶

Magnetic resonance imaging offers several advantages over cardiovascular imaging: its true multiplanar capabilities, its lack of ionizing radiation, its absence of need for an iodinated contrast agent, and its ability not only to characterize shunt direction but also to quantify flow.¹⁷⁻¹⁹ However, its disadvantages include lower spatial resolution, increased pixel size, susceptibility artifacts, and longer examination times. For a series of studies in different planes, such as would produce an overview of the relations between adjacent structures, good and extended breath-holding is required. Thus, MRI for children younger than 5 years of age usually requires sedation or anesthesia. These disadvantages can limit the clinical application of MRI in very young, sick, and noncompliant pediatric patients.

At the present, MDCTA is increasingly used in the evaluation of patients with known or suspected congenital heart disease, especially when accompanying vascular anomalies must be ruled out. The advantages of MDCTA include large imaging areas and rapid data acquisition in a single breath-hold. Multidetector CT might not provide additional diagnostic information about isolated TAPVC; however, it might be assumed to show superiority over TTE and catheter angiography in the evaluation of patients with complex TAPVC.¹⁵ Multidetector CT angiography can yield 2- and 3-dimensional reconstructed images with high spatial resolution, which is helpful in evaluating complex cardiovascular anomalies. Liu and colleagues¹⁵ have shown that MDCTA is superior to TTE and catheter angiography in the evaluation of TAPVC, especially in patients with complex congenital cardiovascular anomalies. The authors reported that MDCTA can distinctly

display the course of anomalous PVs from the periphery, through the hilum and mediastinum, to their drainage sites; and MDCTA is especially useful in detecting abnormal vascular connections outside the usual echocardiographic windows.

In comparison with isolated TAPVC, complex TAPVC has a distinctly less favorable prognosis. When some patients with complex TAPVC present with associated cardiac anomalies other than those usually found in TAPVC patients, the suspicion of accompanying TAPVC might not be raised. If TAPVC is not detected and corrected, it can result in intractable and fatal pulmonary edema, and in difficulty in weaning the patient from cardiopulmonary bypass.¹⁵ Therefore, detailed delineation of complex TAPVC is crucial in surgical planning for these patients. In the present study, MDCTA led to the correct identification of complex TAPVC in all patients.

In patients with obstructive TAPVC, the obstruction can lie within the anomalous connecting vein or at its connection to the systemic circulation. Although obstruction can occur in any type of TAPVC, it is most often encountered in the infracardiac type,²⁰ wherein the PVs drain a confluence posterior to the left atrium. A descending vertical vein originates from this confluence, passes through the esophageal hiatus, and drains below the diaphragm into the portal venous system, the inferior vena cava, the hepatic veins, the ductus venosus, or the azygos vein. The descending vertical vein might be obstructed by extrinsic narrowing, usually at the level of the diaphragm; this can result in neonatal pulmonary edema. Furthermore, when the anomalous connection is to the portal venous system, the high resistance of the hepatic parenchymal circulation creates its own barrier to blood flow for the PV.²⁰

Children with infracardiac TAPVC accounted for 42% of the obstructed veins in our study. In one child, obstruction was at the left hepatic vein-to-inferior vena cava connection; in another child, at the vertical vein-to-ductus venosus connection; and in a third child, at the diaphragmatic level.

In supracardiac TAPVC, the PVs drain a confluence posterior to the left atrium: an ascending vertical vein originates from this confluence, usually passes anterior to the left pulmonary artery, and most often drains into the left brachiocephalic vein. Unusually, the vertical vein passes between the left pulmonary artery and the left bronchus, leading to pulmonary venous obstruction.⁴ Rarely, the site of entrance to the brachiocephalic vein is also narrowed, and this leads to obstruction. In the present study, children with supracardiac TAPVC accounted for 42% of the obstructed veins, and for all obstructions at the entrance to the systemic veins. In cardiac TAPVC, pulmonary venous confluence drains directly into the right atrium, usually through the coronary sinus. Obstruction is unusual in this type of TAPVC.²⁰

Because radiation exposure with MDCTA has become a foremost concern—especially in children, consequential to the risks of radiation-induced chromosomal DNA damage and cancer—every approach to the minimization of radiation dosage (while preserving image quality) is important. One should always apply the principle of “as low as reasonably achievable.” In an average of all age groups, the estimated additional lifetime risk for developing cancer after 10 mSv radiation exposure is approximately 1 in 2,000.¹³ Children have a higher risk of damage from radiation exposure than do adults, because of longer life expectancy and higher radiation sensitivity. Therefore, pediatric scanning protocols with safeguards designed specifically for children are necessary. The latest technologic advances (such as scanners with a high volume of coverage) have enabled sub-mSv doses with acquisitions lasting less than 1 s. These devices can scan the entire thorax without the need for sedation and can obtain volumetric high-resolution images, even in small children who are unable to follow breathing instructions.⁶⁻¹³ The effective radiation doses are similar to those for previously reported acquisitions by scanners with high volumes of coverage. In the study performed by Bonelli-Sica and colleagues⁶ using 256-slice MDCT (whether with ECG-gated or non-ECG-gated protocol) in pediatric patients with anomalous PV drainage, the overall effective radiation dose was 1.01 mSv (range, 0.13–6.43 mSv), and it was 0.78 mSv (range, 0.13–4.16) in patients younger than 1 year of age. In another study—by Huang and associates,⁸ performed by 256-slice MDCT with a prospectively ECG-gated protocol in infants with congenital heart disease—the effective radiation dose was 1.6 ± 0.3 mSv (range, 1.1–2.5 mSv). Al-Mousily and co-authors¹¹ reported that the effective radiation dose in their study, conducted with 320-slice MDCT in infants and young children with congenital heart disease, was 0.8 ± 0.39 mSv (range, 0.4–1.5 mSv).

In the present study, we observed that the average estimated effective radiation dose was 0.66 mSv (range, 0.15–1.11 mSv), and in patients younger than 1 year old it was 0.52 mSv (range, 0.12–0.72). We used a non-ECG-gated protocol in all of our patients, because coronary artery evaluation was not needed. Contrary to recently published studies⁸⁻¹⁰ performed by means of high-volume-of-coverage MDCT scanners with prospectively ECG-gated protocols, our institution's ECG-gated study is reserved for those patients who need coronary artery evaluation. In patients with previously known or suspected TAPVC, who might need a large craniocaudal volume of coverage (from the base of the neck to the inferior portion of the liver), even these low-dose protocols can increase the radiation dose. A dual-source 256-slice MDCT scanner with high-pitch protocol yields a higher temporal resolution. This is important in imaging infants and small children, in order

that acquisitions might be obtained with the patients breathing freely, in the absence of sedation or anesthesia—which is nearly always necessary for MRI.

Limitations of the Study. Our study has some limitations. First, there is the matter of a selection bias: ours is a combined retrospective and prospective study, for which we selected only patients with a diagnosis of TAPVC obtained from MDCT, and from which we excluded patients whose MDCT scans were negative (either true or false negative). Second, the results of the study are those of a single center with substantial experience in the performance of cardiovascular MDCTA. Therefore, it might not be accurate to generalize these results beyond centers that have experience and equipment similar to ours. Indeed a multicenter study is warranted to confirm our results. Third, the effective radiation doses were calculated from the “dose-length product” provided by the scanner’s control unit. The dose-length product is not a directly measured dose value, but an estimation of radiation dose.

In Conclusion. The drainage sites, the presence of obstruction, and the cardiovascular anomalies that accompany TAPVC can be reliably and noninvasively identified by high-pitch dual-source 256-slice MDCTA, with lower radiation doses and without the need for sedation and breath-holding in a pediatric population. Multidetector CT scanners with a high volume of coverage should be used as a second-line investigative method, after TTE, to complete or confirm the diagnosis of TAPVC.

References

1. Karamlou T, Gurofsky R, Al Sukhni E, Coles JG, Williams WG, Caldarone CA, et al. Factors associated with mortality and reoperation in 377 children with total anomalous pulmonary venous connection. *Circulation* 2007;115(12):1591-8.
2. Geva T, van Praagh S. Anomalies of the pulmonary veins. In: Allen HD, Driscoll DJ, Shaddy RE, Feltes TF, editors. Moss and Adams’ heart disease in infants, children, and adolescents: including the fetus and young adult. 7th ed. Philadelphia: Lippincott Williams & Wilkins; 2008. p. 761-92.
3. Caldarone CA, Najm HK, Kadletz M, Smallhorn JF, Freedom RM, Williams WG, Coles JG. Surgical management of total anomalous pulmonary venous drainage: impact of coexisting cardiac anomalies. *Ann Thorac Surg* 1998;66(5):1521-6.
4. Vyas HV, Greenberg SB, Krishnamurthy R. MR imaging and CT evaluation of congenital pulmonary vein abnormalities in neonates and infants. *Radiographics* 2012;32(1):87-98.
5. Delisle G, Ando M, Calder AL, Zuberhuhler JR, Rochenmacher S, Alday LE, et al. Total anomalous pulmonary venous connection: report of 93 autopsied cases with emphasis on diagnostic and surgical considerations. *Am Heart J* 1976; 91(1):99-122.
6. Bonelli-Sica JM, de la Mora-Cervantes R, Diaz-Zamudio M, Castillo-Castellon F, Ramirez-Carmona R, Velazquez-Moreno J, Kimura-Hayama E. Dual-source 256-MDCT for diagnosis of anomalous pulmonary venous drainage in pediatric population. *AJR Am J Roentgenol* 2013;200(2):W163-9.
7. Han BK, Overman DM, Grant K, Rosenthal K, Rutten-Ramos S, Cook D, Lesser JR. Non-sedated, free breathing cardiac CT for evaluation of complex congenital heart disease in neonates. *J Cardiovasc Comput Tomogr* 2013;7(6):354-60.
8. Huang MP, Liang CH, Zhao ZJ, Liu H, Li JL, Zhang JE, et al. Evaluation of image quality and radiation dose at prospective ECG-triggered axial 256-slice multi-detector CT in infants with congenital heart disease. *Pediatr Radiol* 2011;41(7):858-66.
9. Gao Y, Lu B, Hou Z, Yu F, Cao H, Han L, Wu R. Low dose dual-source CT angiography in infants with complex congenital heart disease: a randomized study. *Eur J Radiol* 2012;81(7):e789-95.
10. Klink T, Muller G, Weil J, Dodge-Khatami A, Adam G, Bley TA. Cardiovascular computed tomography angiography in newborns and infants with suspected congenital heart disease: retrospective evaluation of low-dose scan protocols. *Clin Imaging* 2012;36(6):746-53.
11. Al-Mousily F, Shifrin RY, Fricker FJ, Feranec N, Quinn NS, Chandran A. Use of 320-detector computed tomographic angiography for infants and young children with congenital heart disease. *Pediatr Cardiol* 2011;32(4):426-32.
12. Han BK, Lindberg J, Grant K, Schwartz RS, Lesser JR. Accuracy and safety of high pitch computed tomography imaging in young children with complex congenital heart disease. *Am J Cardiol* 2011;107(10):1541-6.
13. Sodhi KS, Krishna S, Saxena AK, Sinha A, Khandelwal N, Lee EY. Clinical application of ‘Justification’ and ‘Optimization’ principle of ALARA in pediatric CT imaging: “how many children can be protected from unnecessary radiation?” *Eur J Radiol* 2015;84(9):1752-7.
14. Thomas KE, Wang B. Age-specific effective doses for pediatric MSCT examinations at a large children’s hospital using DLP conversion coefficients: a simple estimation method. *Pediatr Radiol* 2008;38(6):645-56.
15. Liu J, Wu Q, Xu Y, Bai Y, Liu Z, Li H, Zhu J. Role of MDCT angiography in the preoperative evaluation of anomalous pulmonary venous connection associated with complex cardiac abnormality. *Eur J Radiol* 2012;81(5):1050-6.
16. Kim TH, Kim YM, Suh CH, Cho DJ, Park IS, Kim WH, Lee YT. Helical CT angiography and three-dimensional reconstruction of total anomalous pulmonary venous connections in neonates and infants. *AJR Am J Roentgenol* 2000; 175(5):1381-6.
17. Riesenkaempff EM, Schmitt B, Schnackenburg B, Huebler M, Alexi-Meskishvili V, Hetzer R, et al. Partial anomalous pulmonary venous drainage in young pediatric patients: the role of magnetic resonance imaging. *Pediatr Cardiol* 2009;30(4): 458-64.
18. Festa P, Ait-Ali L, Cerillo AG, De Marchi D, Murzi B. Magnetic resonance imaging is the diagnostic tool of choice in the preoperative evaluation of patients with partial anomalous pulmonary venous return. *Int J Cardiovasc Imaging* 2006;22(5):685-93.
19. Nordmeyer S, Berger F, Kuehne T, Riesenkaempff E. Flow-sensitive four-dimensional magnetic resonance imaging facilitates and improves the accurate diagnosis of partial anomalous pulmonary venous drainage. *Cardiol Young* 2011;21(5):528-35.
20. Shen Q, Pa M, Hu X, Wang J. Role of plain radiography and CT angiography in the evaluation of obstructed total anomalous pulmonary venous connection. *Pediatr Radiol* 2013;43(7):827-35.